Research Article

Solvothermal Synthesis of $Gd_2O_3 : Eu^{3+}$ Luminescent Nanowires

Guixia Liu, Song Zhang, Xiangting Dong, and Jinxian Wang

School of Chemistry and Environmental Engineering, Changchun University of Science and Technology, Changchun 130022, China

Correspondence should be addressed to Guixia Liu, liuguixia22@yahoo.com.cn

Uniform $Gd_2O_3 : Eu^{3+}$ luminescent nanowires were prepared on a large scale by a facile solvothermal method using polyethylene glycol (PEG-2000) as template and ethanol as solvent; the properties and the structure were characterized. X-ray diffraction (XRD) patterns and Fourier transform infrared spectrometry (FTIR) showed that the precursors are hexagonal phase $Gd(OH)_3$ crystals, and the samples calcined at 800°C are cubic phase Gd_2O_3. Transmission Electron Microscopy (TEM) images indicated that the samples are nanowires with a diameter of 30 nm and a length of a few microns. Photoluminescence (PL) spectra showed that the ratio of $^5D_0 \rightarrow {}^7F_2$ to $^5D_0 \rightarrow {}^7F_1$ transition peak of the calcined samples is stronger than that of the precursors, which confirmed that the color purity of the $Gd_2O_3 : Eu^{3+}$ is better than that of the precursors. The as-obtained $Gd_2O_3 : Eu^{3+}$ luminescent nanowires show a strong red emission corresponding to $^5D_0 \rightarrow {}^7F_2$ transition (610 nm) of Eu^{3+} under ultraviolet excitation (250 nm), which have potential application in red-emitting phosphors and field emission display devices.

1. Introduction

Recently, 1D nanomaterials have been attracted much attention for their unique properties owing to their low dimension and high surface/volume ratio; therefore, they have potential applications in fabricating nanoscale electronic, optoelectronic, and magnetic devices and also provide an ideal model system to quantized conductance and size effects [1]. 1D rare earth oxide nanomaterials are a kind of advanced materials and have extensive applications on the fields of high-performance luminescent devices, catalysts, and other functional materials for their special electronic, optical, and chemical characteristics arising from their 4f electron. Several strategies have been developed for preparing 1D rare earth oxide nanomaterials, including template method [2–7], hydrothermal or solvothermal method [8–18], and chemical reaction [19–22]. Among these methods, the hydrothermal or solvothermal techniques are powerful and important means to synthesize 1D rare earth oxide nanomaterials due to their great chemical flexibility and synthetic tenability.

As well known, in rare earth oxide luminescence materials, Europium-doped Gd_2O_3 phosphor is one of the most important red-emitting phosphors and has been widely used in X-ray scintillator materials, high definition projection televisions, flat panel displays, and photoelectronic apparatus [23]. Over the past decade, $Gd_2O_3 : Eu^{3+}$ nanoparticles had been investigated extensively [24–27]. When $Gd_2O_3 : Eu^{3+}$ is prepared in the form of one-dimensional nanomaterials such as nanowires, nanorods or, nanotubes, its application would be widely extended due to the shape-specific and quantum confinement effects. However, compared with the study of $Gd_2O_3 : Eu^{3+}$ nanoparticles, there have been few reports on the synthesis of 1D $Gd_2O_3 : Eu^{3+}$ nanomaterials; for example, Jia et al. [19] had prepared $Gd_2O_3 : Eu^{3+}$ nanotubes via a wet-chemical route and a subsequent heat-treatment. Li et al. [28] had prepared $Gd_2O_3 : Eu^{3+}$ nanowires via AAO templated method, the method is complex, and the size of the obtained samples is limited by the template. Zhang et al. [29] had prepared $Gd_2O_3 : Eu^{3+}$ nanorods by surfactant-assisted hydrothermal method. Liu et al. [30] used MWCNTs as a template, coating gadolinium compounds on the carbon nanotube surface, followed by firing the carbon nanotube to obtain the $Gd_2O_3 : Eu^{3+}$ nanotubes, but the MWCNT template was difficult to remove afterwards. Herein, a large-scale uniform $Gd_2O_3 : Eu^{3+}$ nanowires were successfully prepared by a simple solvothermal method at the presence of polyethylene glycol followed by a subsequent calcination process, and the structure and properties were characterized.
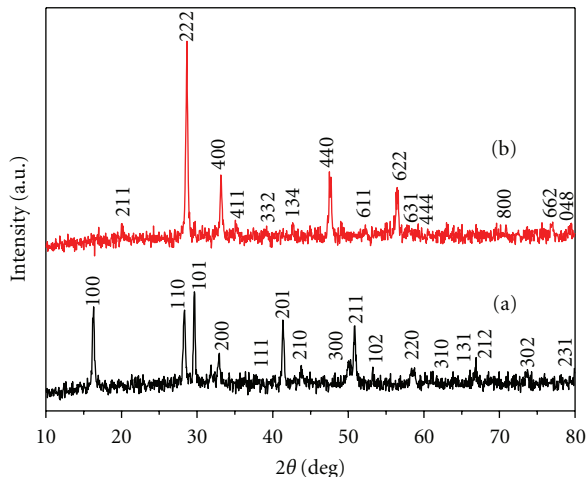
Figure 1: XRD patterns of the precursors (a) and the samples annealing at 800°C (b).

Figure 2: FTIR spectra of the precursors (a) and the samples annealing at 800°C (b).

2. Experimental Section

2.1. Preparation.
In a typical synthesis, first, 4.5349 g Gd_2O_3 and 1.7608 g Eu_2O_3 (purity: 99.99%, Shanghai Yuelong Non-Ferrous Metals Limited, China) were dissolved in a minimum amount of diluted nitric acid ($V_{HNO_3} : V_{H_2O} = 1 : 1$) and evaporated to dryness then dissolved in distilled water to form $0.1 \, mol \cdot L^{-1}$ gadolinium nitrate and $0.05 \, mol \cdot L^{-1}$ europium nitrate solutions.

Secondly, 30 mL absolute ethanol and 12.8 g polyethylene glycol (PEG, A.R., molecular weight is 2000, Shanghai Linger Chemical Company, China) were added into the mixture of a certain amount of $Gd(NO_3)_3$ and $Eu(NO_3)_3$ solutions according to the molar ratio of Gd/Eu = 95 : 5, in which the molar ratio of rare earth ion and the surfactant PEG is 1 : 2. And then $4 \, mol \cdot L^{-1}$ NaOH was added to adjust pH of 13; after being stirred for 30 minutes, the mixture was transferred into a 50 mL autoclave, sealed and heated at 180°C for 48 hours. After the autoclave was cooled to room temperature naturally, the precursors were filtered and washed with distilled water and absolute ethanol for three times, respectively. The final white products were obtained through a heat-treatment at 800°C in air for 2 hours after being dried at 80°C for 2 hours.

2.2. Characterization.
The sample crystal structure was characterized by an Aolong Y-2000 X-ray Diffractometer (XRD) equipped with a Cu $K_{\alpha 1}$ radiation source ($\lambda = 0.154056 \, nm$) and Ni filter at a scanning rate of $4° \cdot min^{-1}$ (2θ from 10 to 80°), X-ray tube voltage and current were 40 kV and 20 mA, respectively, and the step was 0.02°. FTIR spectra were measured with Perkin-Elmer 580B Infrared Spectrophotometer with the KBr pellet technique. The morphologies of the samples and the selected area electron diffraction (SAED) pattern were observed using a JEOL JEM-2010 Transmission Electron Microscopy (TEM), and the voltage was 160 kV. Photoluminescence (PL) excitation and emission spectra of the samples were recorded with a
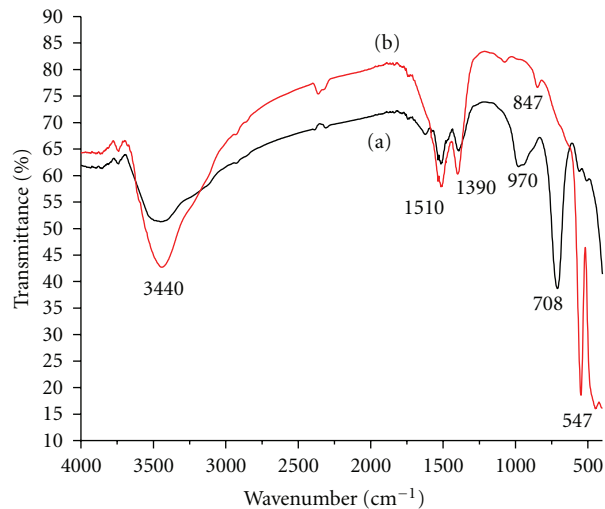
HITACHI F-4500 Fluorescence Spectrophotometer using a Xe lamp as the excitation source, the measurement range is 200–800 nm, scanning rate is 1200 nm/min, and step length is 0.2 nm. All the measurements were performed at room temperature.

3. Results and Discussion

3.1. XRD Patterns.
XRD patterns of the precursors and the calcined samples are shown in Figure 1, it is noted that the precursors are well indexed to be a pure hexagonal phase $Gd(OH)_3$, identical to the reported data in JCPDS card (83-2037), because the Eu content is low, there are no peaks of $Eu(OH)_3$, and the cell constants of $Gd(OH)_3$ are almost not changed. After annealing at the temperature of 800°C, the intensities and the positions of the peaks are all changed, and the diffraction peaks are coincided with the data of JCPDS card of (12-0797), which indicated that the calcined samples are pure cubic phase Gd_2O_3. Moreover, it can be observed that the diffraction peaks of the calcined samples are very sharp and strong, indicating that the Gd_2O_3 samples with high crystallinity are synthesized by this method.

3.2. FTIR Spectra.
Figure 2 shows the FTIR spectra of the precursors and the calcined samples; from Figure 2(a), the absorption peak at $3440 \, cm^{-1}$ is due to vibration of –OH in H_2O, and the peaks at $1510 \, cm^{-1}$ and $1390 \, cm^{-1}$ are ascribed to the vibration of NO_3^- [31], which originated from the residue NO_3^- in the sample. The peak near $703 \, cm^{-1}$ is designed to vibration of Gd–OH, which indicated that the precursors are $Gd(OH)_3$. From Figure 2(b), it can be seen that the absorption peaks at $3440 \, cm^{-1}$, $1510 \, cm^{-1}$ and $1390 \, cm^{-1}$ are stronger than those of the precursors; it is reported that the peaks in the wavelength range of 1400–1600 come from the carbonate groups and a weak peak at $847 \, cm^{-1}$ is due to the absorption of CO_3^{2-} [32]. Perhaps

(a)

(b)

(c)

Figure 3: TEM images of the calcined samples ((a), low magnification (b), high magnification) with its SAED pattern (c).

the samples absorbed the CO_2 and H_2O from the atmosphere during the measurement process and the storage course, and which led to the overlap of CO_3^{2-} and the residue NO_3^{-}. The important absorption peak at $547\,cm^{-1}$ is ascribed to vibration of Gd–O, suggesting that the $Gd(OH)_3$ had

converted to Gd_2O_3 after calcinating; this result confirms the analysis from XRD patterns.

3.3. TEM Images. In order to study the morphology and the size of the as-prepared $Gd_2O_3 : Eu^{3+}$ nanomaterials, the samples were investigated by TEM, which are shown in Figures 3(a) and 3(b). It is seen clearly that the samples comprise wire shapes and are generally well dispersed. The diameter of the wires is about 30 nm and the length reaches to micrometer scale. It is also observed that the samples are smooth and uniform. Figure 3(c) is the corresponding SAED pattern; one can see the (211), (222), (400), and (440) planes of the cubic phase Gd_2O_3, which is in agreement with the XRD results.

3.4. Photoluminescence Spectra. The uniform $Gd_2O_3 : Eu$ nanowires obtained by the solvothermal method exhibit a strong red emission under short UV irradiation, and the spectral properties are typical of the well-known $Gd_2O_3 : Eu$ [24, 25, 27].

The excitation spectra of the precursors and the samples calcined at 800°C are drawn in Figure 4; the monitoring wavelength is $^5D_0$–$^7F_2$ transition at 610 nm of the Eu^{3+}. It is noted that the excitation peaks of the precursors are weaker than those of the calcined samples. From the magnified spectrum of the inset, it is obvious that the strong excitation peak is near 250 nm, which originated from the charge transfer band of O^{2-}–Eu^{3+}, and the weak peak near 394 nm is due to the $^7F_0 \rightarrow {}^5L_6$ transition of Eu^{3+}. After being calcined at 800°C, the excitation spectrum becomes stronger and it consists of an intense broad band near 232 and 247 nm, the former is due to the host absorption of Gd_2O_3, and the latter is attributed to the charge transfer band (CTB) of O^{2-}–Eu^{3+} [33]. The weak shoulder at 276 nm superimposed on the CTB of Eu^{3+} can be assigned to the ^8S–^6I transition line of Gd^{3+} [34]. The presence of the Gd_2O_3 host band and Gd^{3+} excitation line in the excitation spectrum of Eu^{3+} indicates that there exists an energy transfer from the Gd_2O_3 host band and Gd^{3+} to the doped Eu^{3+} [34]. At the same time, a serious of weak intensity peaks near 314 nm, 394 nm, and 465 nm can be seen, which is supported to the $^7F_0 \rightarrow {}^5H_6$, $^7F_0 \rightarrow {}^5L_6$, $^7F_0 \rightarrow {}^5D_2$ energy level transition of Eu^{3+} [34, 35].

Figure 5 shows the emission spectra of the precursors and the calcined samples, the excitation wavelength is the CTB of Eu^{3+} at 250 nm. From the magnified spectrum of the precursors, it can be seen that the emission spectrum consists of $^5D_0 \rightarrow {}^7F_j$ ($j = 0, 1, 2$) line emissions of Eu^{3+}, the strongest emission peak is near 610 nm, which corresponds to the hypersensitive $^5D_0 \rightarrow {}^7F_2$ transition of Eu^{3+}, and the line peak at 590 nm is due to $^5D_0 \rightarrow {}^7F_1$ magnetic dipole transition, which emits orange red light. After being calcined at 800°C, the emission spectrum consists of $^5D_{0,1} \rightarrow {}^7F_J$ ($J = 0, 1, 2, 3, 4$) line peaks of Eu^{3+}, that is 532 nm ($^5D_1 \rightarrow {}^7F_1$), 578 nm ($^5D_0 \rightarrow {}^7F_0$), 586, 590, 596 nm ($^5D_0 \rightarrow {}^7F_1$), 610, 626 nm ($^5D_0 \rightarrow {}^7F_2$), 647 nm ($^5D_0 \rightarrow {}^7F_3$) and 704 nm ($^5D_0 \rightarrow {}^7F_4$) [33–35]. The strongest emission peak is also at 610 nm ($^5D_0 \rightarrow {}^7F_2$), which is the characteristic red emission of Eu^{3+}. In contrast to the peak

FIGURE 4: Excitation spectra of the precursors and the samples annealing at $800°C$ (the inset is the magnified spectrum of the precursors).
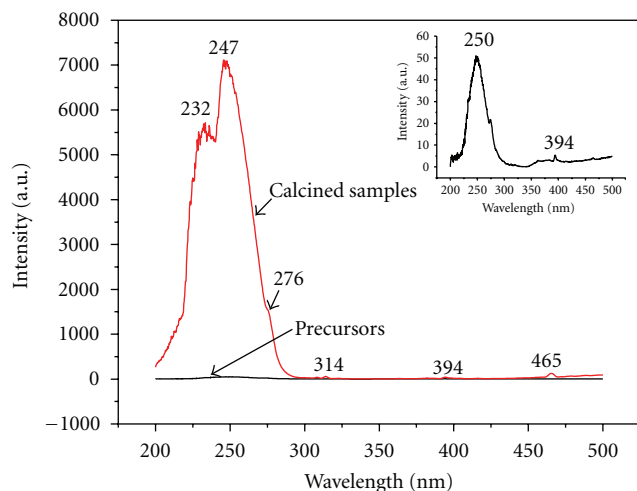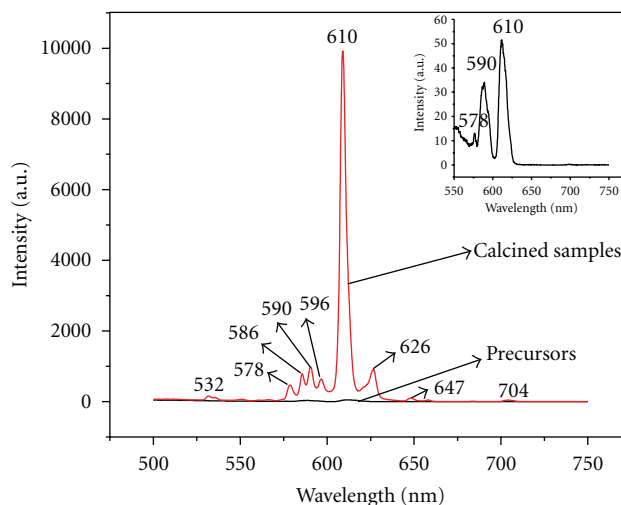

FIGURE 5: Emission spectra of the precursors and the samples annealing at $800°C$ (the inset is the magnified spectrum of the precursors).

of 610 nm ($^5D_0 \rightarrow ^7F_2$), the peak at 590 nm ($^5D_0 \rightarrow ^7F_1$) is very weak. According to the selection rules and transition probabilities, $^5D_0 \rightarrow ^7F_2$ electron dipole transition is the strongest emission when Eu^{3+} is located at a noninversion symmetry site. In a site with inversion symmetry the $^5D_0 \rightarrow ^7F_1$ magnetic dipole transition is dominant. It is known that the ratio of $^5D_0 \rightarrow ^7F_2$ (red light) to $^5D_0 \rightarrow ^7F_1$ (orange red light) can be used to confirm the red color purity of the phosphors. Comparing the emission spectra of the precursors with the calcined samples, it is found that the ratio of $^5D_0 \rightarrow ^7F_2$ to $^5D_0 \rightarrow ^7F_1$ of the calcined samples is larger than that of the precursors, which confirmed that as red luminescence materials, the color purity of $Gd_2O_3 : Eu^{3+}$ is superior to that of $Gd(OH)_3 : Eu^{3+}$, and also suggesting that as luminescence host, Gd_2O_3 is better than $Gd(OH)_3$.

From the luminescence spectra, one can see that the intensity of the calcined samples ($Gd_2O_3 : Eu^{3+}$) is much stronger than that of the precursors ($Gd(OH)_3 : Eu^{3+}$); it is supported that, in the precursors, the –OH group originated from $Gd(OH)_3 : Eu^{3+}$, absorption surface H_2O and the impurities on the samples' surface are served as the quenching center for the luminescent materials, which decrease the intensity of the precursors. After the annealing process, the $Gd(OH)_3$ converted to $Gd_2O_3 : Eu^{3+}$, and the impurities dramatically decreased, which resulted in the increase of the intensity of the calcined samples.

4. Conclusion

In summary, large-scale $Gd_2O_3 : Eu^{3+}$ luminescent nanowires have been successfully synthesized by a facile solvothermal method and followed by a subsequent heat-treatment. The morphology, crystal structure, and luminescence properties were characterized by TEM, XRD, FTIR, and PL. The results showed that the precursors are hexagonal phase $Gd(OH)_3$ and the calcined samples are pure cubic phase Gd_2O_3. The

as-obtained $Gd_2O_3 : Eu^{3+}$ luminescent nanowires have the diameter of 30 nm and can stretch to micrometer lengths. The ratio of $^5D_0 \rightarrow ^7F_2$ to $^5D_0 \rightarrow ^7F_1$ for the intensity of the calcined sample is stronger than that of the precursors, confirming that the color purity of $Gd_2O_3 : Eu^{3+}$ is better than that of $Gd(OH)_3 : Eu^{3+}$ for red phosphors. The as-prepared $Gd_2O_3 : Eu^{3+}$ luminescent nanowires are potentially applied in red-emitting phosphors and field emission display devices. This facile method can be used to synthesize other rare earth oxide luminescence materials.

Acknowledgments

References

[1] Y. Tian, Y. He, and Y. Zhu, "Low temperature synthesis and characterization of molybdenum disulfide nanotubes and nanorods," *Materials Chemistry and Physics*, vol. 87, no. 1, pp. 87–90, 2004.

[2] G. Wu, L. Zhang, B. Cheng, T. Xie, and X. Yuan, "Synthesis of Eu_2O_3 nanotube arrays through a facile sol-gel template approach," *Journal of the American Chemical Society*, vol. 126, no. 19, pp. 5976–5977, 2004.

[3] M. Yada, M. Mihara, S. Mouri, M. Kuroki, and T. Kijima, "Rare earth (Er, Tm, Yb, Lu) oxide nanotubes templated by dodecylsulfate assemblies," *Advanced Materials*, vol. 14, no. 4, pp. 309–313, 2002.

[4] A. Vantomme, Z.-Y. Yuan, G. Du, and B.-L. Su, "Surfactant-assisted large-scale preparation of crystalline CeO_2 nanorods," *Langmuir*, vol. 21, no. 3, pp. 1132–1135, 2005.

[5] J. Zhang and G. Hong, "Synthesis and photoluminescence of the Y_2O_3:Eu^{3+} phosphor nanowires in AAO template," *Journal of Solid State Chemistry*, vol. 177, no. 4-5, pp. 1292–1296, 2004.

[6] C. Wu, W. Qin, G. Qin, D. Zhao, J. Zhang, S. Huang, S. Lü, H. Liu, and H. Lin, "Photoluminescence from surfactant-assembled Y_2O_3:Eu nanotubes," *Applied Physics Letters*, vol. 82, no. 4, pp. 520–523, 2003.

[7] G. Liu and G. Hong, "Synthesis and photoluminescence of Y_2O_3:RE^{3+}(RE = Eu, Tb, Dy) porous nanotubes templated by carbon nanotubes," *Journal of Nanoscience and Nanotechnology*, vol. 6, no. 1, pp. 120–124, 2006.

[8] X. Bai, H. Song, L. Yu, L. Yang, Z. Liu, G. Pan, S. Lu, X. Ren, Y. Lei, and L. Fan, "Luminescent properties of pure cubic phase Y_2O_3/Eu^{3+} nanotubes/nanowires prepared by a hydrothermal method," *Journal of Physical Chemistry B*, vol. 109, no. 32, pp. 15236–15242, 2005.

[9] Y. Mao, J. Y. Huang, R. Ostroumov, K. L. Wang, and J. P. Chang, "Synthesis and luminescence properties of erbium-doped Y_2O_3 nanotubes," *Journal of Physical Chemistry C*, vol. 112, no. 7, pp. 2278–2285, 2008.

[10] X. Wang and Y. Li, "Synthesis and characterization of lanthanide hydroxide single-crystal nanowires," *Angewandte Chemie - International Edition*, vol. 41, no. 24, pp. 4790–4793, 2002.

[11] Q. Tang, J. Shen, W. Zhou, W. Zhang, W. Yu, and Y. Qian, "Preparation, characterization and optical properties of terbium oxide nanotubes," *Journal of Materials Chemistry*, vol. 13, no. 12, pp. 3103–3106, 2003.

[12] X. Wu, Y. Tao, F. Gao, L. Dong, and Z. Hu, "Preparation and photoluminescence of yttrium hydroxide and yttrium oxide doped with europium nanowires," *Journal of Crystal Growth*, vol. 277, no. 1–4, pp. 643–649, 2005.

[13] B. Tang, J. Ge, and L. Zhuo, "The fabrication of $La(OH)_3$ nanospheres by a controllable-hydrothermal method with citric acid as a protective agent," *Nanotechnology*, vol. 15, no. 12, pp. 1749–1753, 2004.

[14] X. Wang and Y. Li, "Rare-earth-compound nanowires, nanotubes, and fullerene-like nanoparticles: synthesis, characterization, and properties," *Chemistry*, vol. 9, no. 22, pp. 5627–5635, 2003.

[15] X. Wang, X. Sun, D. Yu, B. Zou, and Y. Li, "Rare earth compound nanotubes," *Advanced Materials*, vol. 15, no. 17, pp. 1442–1445, 2003.

[16] M. H. Zahir, T. Suzuki, Y. Fujishiro, and M. Awano, "Synthesis and characterization of Sm^{3+}-doped $Y(OH)_3$ and Y_2O_3 nanowires and their NO reduction activity," *Journal of Alloys and Compounds*, vol. 476, no. 1-2, pp. 335–340, 2009.

[17] Z. Xu, Z. Hong, Q. Zhao, L. Peng, and P. Zhang, "Preparation and luminescence properties of Y_2O_3:Eu^{3+} nanorods via post annealing process," *Journal of Rare Earths*, vol. 24, no. 2, pp. 111–114, 2006.

[18] G. Jia, Y. H. Zheng, K. Liu, Y. H. Song, H. P. You, and H. J. Zhang, "Facile surfactant- and template-free synthesis and luminescent properties of one-dimensional Lu_2O_3:Eu^{3+} phosphors," *Journal of Physical Chemistry C*, vol. 113, no. 1, pp. 153–158, 2009.

[19] G. Jia, K. Liu, Y. Zheng, Y. Song, M. Yang, and H. You, "Highly uniform $Gd(OH)_3$ and Gd_2O_3:Eu^{3+} nanotubes: facile synthesis and luminescence properties," *Journal of Physical Chemistry C*, vol. 113, no. 15, pp. 6050–6055, 2009.

[20] N. Du, H. Zhang, X. Ma, D. Li, and D. Yang, "Controllable chemical reaction synthesis of $Tb(OH)_3$ nanorods and their photoluminescence property," *Materials Letters*, vol. 63, no. 13-14, pp. 1180–1182, 2009.

[21] N. Du, H. Zhang, B. Chen, J. Wu, D. Li, and D. Yang, "Low temperature chemical reaction synthesis of single-crystalline $Eu(OH)_3$ nanorods and their thermal conversion to Eu_2O_3 nanorods," *Nanotechnology*, vol. 18, no. 6, Article ID 065605, 2007.

[22] N. Du, H. Zhang, B. Chen, X. Ma, and D. Yang, "Ligand-free self-assembly of ceria nanocrystals into nanorods by oriented attachment at low temperature," *Journal of Physical Chemistry C*, vol. 111, no. 34, pp. 12677–12680, 2007.

[23] A. Bril and W. L. Wanmaker, "Fluorescent properties of some europium-activated phosphors," *Journal of Electrochemistry Society*, vol. 111, pp. 1363–1368, 1964.

[24] Y. Li, G. Liu, and G. Hong, "Synthesis and luminescence properties of Gd_2O_3:Eu^{3+} phosphors," *Journal of Rare Earths*, vol. 22, no. 1, pp. 70–74, 2004.

[25] B. Mercier, C. Dujardin, G. Ledoux, C. Louis, O. Tillement, and P. Perriat, "Observation of the gap blueshift on Gd_2O_3:Eu^{3+} nanoparticles," *Journal of Applied Physics*, vol. 96, no. 1, pp. 650–653, 2004.

[26] G.-X. Liu, G.-Y. Hong, and D.-X. Sun, "Preparation of spherical nanometer Gd_2O_3:Eu luminescent materials," *Chinese Journal of Inorganic Chemistry*, vol. 20, no. 11, pp. 1367–1370, 2004 (Chinese).

[27] G.-X. Liu, J.-X. Wang, X.-T. Dong, and G.-Y. Hong, "Gd_2O_3:Eu^{3+} luminescent nano-materials prepared by sol-lyophilization method," *Journal of Inorganic Materials*, vol. 22, no. 5, pp. 803–806, 2007 (Chinese).

[28] S. Li, H. Song, H. Yu, S. Lu, X. Bai, G. Pan, Y. Lei, L. Fan, and T. Wang, "Influence of annealing temperature on photoluminescence characteristics of Gd_2O_3:Eu/AAO nanowires," *Journal of Luminescence*, vol. 122-123, no. 1-2, pp. 876–878, 2007.

[29] S. Zhang, G.-X. Liu, X.-T. Dong, J.-X. Wang, and H. Y. Bao, "Preparation and photoluminescence properties of Gd_2O_3:Eu^{3+} nanorods," *Chemical Journal of Chinese Universities*, vol. 30, no. 1, pp. 7–10, 2009 (Chinese).

[30] G. Liu, G. Hong, X. Dong, and J. Wang, "Preparation and characterization of Gd_2O_3:Eu^{3+} luminescence nanotubes," *Journal of Alloys and Compounds*, vol. 466, no. 1-2, pp. 512–516, 2008.

[31] Z. Xu, J. Yang, Z. Hou, C. Li, C. Zhang, S. Huang, and J. Lin, "Hydrothermal synthesis and luminescent properties of Y_2O_3:Tb^{3+} and Gd_2O_3:Tb^{3+} microrods," *Materials Research Bulletin*, vol. 44, no. 9, pp. 1850–1857, 2009.

[32] C. Louis, R. Bazzi, M. A. Flores, W. Zheng, K. Lebbou, O. Tillement, B. Mercier, C. Dujardin, and P. Perriat, "Synthesis and characterization of Gd_2O_3:Eu^{3+} phosphor nanoparticles by a sol-lyophilization technique," *Journal of Solid State Chemistry*, vol. 173, no. 2, pp. 335–341, 2003.

[33] M. L. Pang, J. Lin, J. Fu, R. B. Xing, C. X. Luo, and Y. C. Han, "Preparation, patterning and luminescent properties of nanocrystalline Gd_2O_3:A(A = Eu^{3+},Dy^{3+},Sm^{3+},Er^{3+}) phosphor films via Pechini sol-gel soft lithography," *Optical Materials*, vol. 23, no. 3-4, pp. 547–558, 2003.

[34] J. Yang, C. Li, Z. Cheng, X. Zhang, Z. Quan, C. Zhang, and J. Lin, "Size-tailored synthesis and luminescent properties of one-dimensional Gd_2O_3:Eu^{3+} nanorods and microrods," *Journal of Physical Chemistry C*, vol. 111, no. 49, pp. 18148–18154, 2007.

[35] J. Yang, Z. Quan, D. Kong, X. Liu, and J. Lin, "Y_2O_3:Eu^{3+} microspheres: solvothermal synthesis and luminescence properties," *Crystal Growth and Design*, vol. 7, no. 4, pp. 730–735, 2007.